

Ferroelectricity and Electronic Structure of Sm-Doped SrBi₂Ta₂O₉ Ceramics

Tohru Higuchi, Shigetaka Watanabe, Nobumasa Ohtake and Takeyo Tsukamoto

Department of Applied Physics, Tokyo University of Science, Tokyo 162-8601, Japan

Fax: +81-3-5228-8241, e-mail: higuchi@rs.kagu.tus.ac.jp

Ferroelectric properties for dense bulk ceramics of Sm-doped SrBi₂Ta₂O₉ (Sm_xSr_{1-x}Bi₂Ta₂O₉) were investigated, and their electronic structures were measured by X-ray absorption spectroscopy (XAS) and soft-X-ray emission spectroscopy (SXES). The remanent polarization (P_r) and coercive field (E_c) depend on the Sm concentration. The P_r and E_c at $x=0.10$ were $2P_r=20.7 \mu\text{C}/\text{cm}^2$ and $2E_c=30.0 \text{ kV}/\text{cm}$, respectively. The valence band of SrBi₂Ta₂O₉ is mainly composed of O 2*p* state hybridized with Ta 5*d* and Bi 6*s* states. The intensity of Bi 6*s* state located at the top of the valence band increases with increasing x . This finding indicates that the Bi³⁺ with lone-pair 6*s* electrons is closely related with the ferroelectricity of SrBi₂Ta₂O₉.

Key words: Sm-doped SrBi₂Ta₂O₉, ceramics, ferroelectricity, electronic structure, hybridization effect

1. INTRODUCTION

Ferroelectric SrBi₂Ta₂O₉ is a member of the Bi-layered Aurivillius family and has a structure in which perovskite Sr-Ta-O layers are sandwiched between Bi-O layers. The crystal structure has orthorhombic distortion with space group $A2_1am$ ($a=0.5522 \text{ nm}$, $b=0.5524 \text{ nm}$ and $c=2.5026 \text{ nm}$) and exhibits large anisotropy [1,2]. The structural distortion with this noncentrosymmetric space group is responsible for the displacive-type ferroelectric behavior. From the viewpoint of crystal structure, SrBi₂Ta₂O₉ has ferroelectricity along the a -axis but not along the c -axis. The SrBi₂Ta₂O₉ thin films are expected for application in memory devices because of its excellent fatigue endurance [3-6].

It is well known that the substitution of Bi³⁺ at the Sr²⁺ site in Sr_{1-x}Bi_{2+x}Ta₂O₉ is effective for improving the ferroelectric properties. The structural and ferroelectric properties have been extensively studied by Shimakawa *et al.* and Noguchi *et al.* [7-12]. The lattice parameter and volume decrease with increasing x , since the ionic radius of Bi³⁺ is smaller than that of Sr²⁺ [12]. The Curie temperature (T_c) increases with increasing Bi³⁺ concentration. The remanent polarization ($2P_r$) increases rapidly from $15 \mu\text{C}/\text{cm}^2$ to $20 \mu\text{C}/\text{cm}^2$ at $x < 0.05$, though the $2P_r$ is constant at $x > 0.05$ [10]. The similar behaviors have been also observed in ABi₂Ta₂O₉ ($A=\text{Ca}, \text{Sr}, \text{and Ba}$) [9,12]. These findings indicate that the Sr²⁺ site strongly affects ferroelectric properties. Miura *et al.* proved the substitution of Bi at the Sr site in Sr_{1-x}Bi_{2+x}Ta₂O₉ on the electronic state calculation by discrete variational X α method and proposed that the Bi ion occupy the Sr site as divalent ions [8]. Furthermore, Noguchi *et al.* also suggested that the T_c tends to change when Bi³⁺ with lone-pair 6*s* electrons occupy the Sr site of the perovskite block [10]. However, the existence of Bi 6*s* state has not been experimentally clarified thus far.

In this work, we have prepared the dense bulk ceramics of Sm-doped SrBi₂Ta₂O₉ (Sm_xSr_{1-x}Bi₂Ta₂O₉) and studied its electronic structure by X-ray absorption spectroscopy (XAS) and soft-X-ray emission spectroscopy (SXES). The SXES and XAS techniques

can confirm the electronic structure of the bulk state, because the mean free path of a soft-X-ray is very long compared with that of an electron. The SXES and XAS spectra, which have a clear selection rule regarding the angular momentum due to dipole transition, reflect the occupied partial-density-of-state (PDOS) and unoccupied PDOS, respectively. Thus, we have observed the change of electronic structure with Sm substitution by means of O 1*s* SXES and XAS techniques.

2. EXPERIMENTAL

Sm_xSr_{1-x}Bi₂Ta₂O₉ ($x=0.05, 0.10$ and 0.20) ceramics were prepared by conventional solid-state reaction method. Powders of Sm₂O₃, SrCO₃, Bi₂O₃, and Ta₂O₅ of 99.99% purity were mixed. The powder calcined at 800°C for 7h was crushed and then pressed into pellets. These pellets were sintered at 1200°C for 4h for ferroelectric, XAS and SXES measurements. The Sm substitution into SrBi₂Ta₂O₉ led to a high relative density of 98%. The structural properties of these ceramics were characterized by X-ray diffraction (XRD) using CuK α . The polarization-electric field (P - E) hysteresis loops were observed using a conventional Sawyer-Tower circuit with a sinusoidal field.

XAS and SXES spectra were measured using a soft-X-ray spectrometer installed at the undulator beamline BL-19B (in Photon Factory) at the High Energy Accelerator Organization [13-16]. Synchrotron radiation was monochromatized using a varied-line spacing plain grating whose average groove density is 1000 lines/mm. The spectra were measured in a polarized configuration. The resolution of about $\Delta E/E=2 \times 10^{-4}$ at $h\nu=400 \text{ eV}$ and high photon flux of about $10^{12} \sim 10^{13}$ photons/sec were realized with the spot size of 100 μm . The XAS spectra were measured by Si photodiode. The SXES spectra were measured by soft-X-ray emission spectrometer. The total resolutions of SXES and XAS were approximately 0.4 eV and 0.1 eV, respectively. The incidence angle of soft-X-ray was about 90° against the surface in order to avoid the surface effect. The bottom axis was

calibrated by measuring the 4f core level of Au film. The spectral intensity was normalized by measurement time and beam current.

The band structure of $\text{SrBi}_2\text{Ta}_2\text{O}_9$ was calculated using tight-binding method [17]. The highly simplified orbital basis sets is used to bring out the main features of the bonding. This calculation uses an orthogonal basis of O 2p, Ta 5d, and Bi 6s and 6p orbital states. The Sr orbital does not use since the Sr 4p and Sr 4d orbital states do not exist in both valence band and conduction band regions. The interaction parameters were found by transferring them from established band structure of related compounds. Two center interactions generally scale with bond length d as d^{-n} , where n varies with the orbital symmetry. The pd interactions scale as $r_d^{3/2}/d^{7/2}$, where r_d is the transition metals d core radius. The Bi-O interactions for the $(\text{Bi}_2\text{O}_2)^{2+}$ layer are scaled as the bond length between Bi and O.

3. RESULTS AND DISCUSSION

Figure 1 shows the XRD patterns as a function of Sm concentration in $\text{Sm}_x\text{Sr}_{1-x}\text{Bi}_2\text{Ta}_2\text{O}_9$ ceramics. These XRD patterns exhibit the single phase. The apparent change of the lattice parameter is not observed in this doping region. For Nd-doped $\text{SrBi}_2\text{Ta}_2\text{O}_9$, it has been reported that the lattice parameter and volume decrease with increasing Nd concentration [12]. Such a situation might be expected for $\text{Sm}_x\text{Sr}_{1-x}\text{Bi}_2\text{Ta}_2\text{O}_9$. The detailed results of structural analysis will be published elsewhere [16].

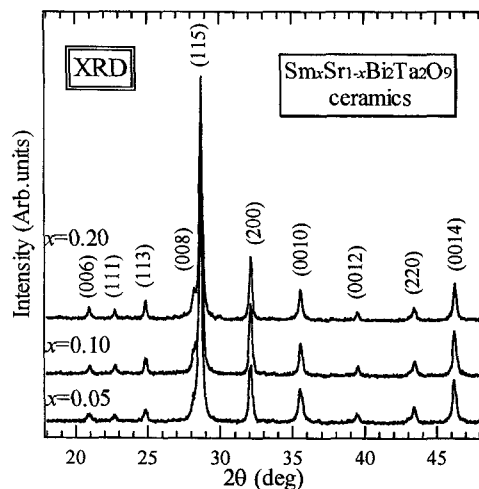


Fig.1 XRD patterns as a function of Sm concentration in $\text{Sm}_x\text{Sr}_{1-x}\text{Bi}_2\text{Ta}_2\text{O}_9$ ceramics.

Figure 2 shows the P - E hysteresis loops as a function of Sm concentration in $\text{Sm}_x\text{Sr}_{1-x}\text{Bi}_2\text{Ta}_2\text{O}_9$ ceramics. The P - E hysteresis loops are observed in all Sm concentrations. In particular, the sample of $x=0.10$ is characterized by a well-saturated P - E hysteresis loop. The P_r of $x=0.05$, 0.10, and 0.20 were $2P_r = 26.5 \mu\text{C}/\text{cm}^2$, $20.7 \mu\text{C}/\text{cm}^2$ and $27.6 \mu\text{C}/\text{cm}^2$, respectively. These values of $\text{Sm}_x\text{Sr}_{1-x}\text{Bi}_2\text{Ta}_2\text{O}_9$ ceramics are larger than those of stoichiometric $\text{SrBi}_2\text{Ta}_2\text{O}_9$ ceramics and thin films [10]. The E_c of $x=0.05$, 0.10, and 0.20 were

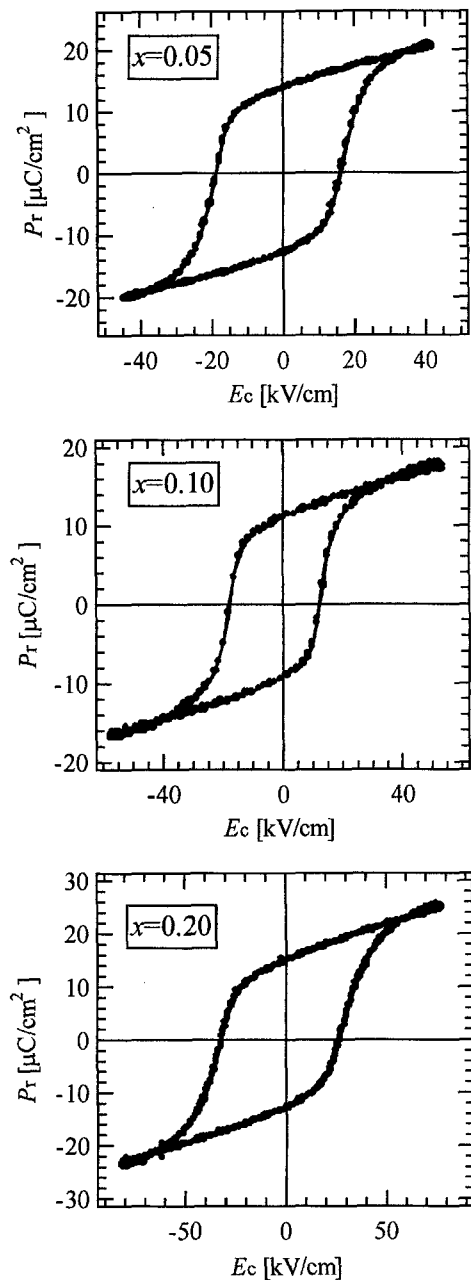


Fig. 2 P - E hysteresis loops as a function of Sm concentration in $\text{Sm}_x\text{Sr}_{1-x}\text{Bi}_2\text{Ta}_2\text{O}_9$ ceramics.

$2E_c = 35.3 \text{ kV}/\text{cm}$, $30.0 \text{ kV}/\text{cm}$ and $59.2 \text{ kV}/\text{cm}$, respectively. The small E_c and large P_r are considered to be due to effect of Sr or Bi site with Sm substitution.

Figure 3 shows the O 1s XAS spectra of $\text{SrBi}_2\text{Ta}_2\text{O}_9$ and $\text{Sm}_{0.10}\text{Sr}_{0.90}\text{Bi}_2\text{Ta}_2\text{O}_9$ ceramics. The XAS spectra are normalized by the Sr 4d peak of the conduction band, though the peak is not shown in this figure. From the dipole selection rule, it is understood that the O 1s XAS spectra of Ta oxides correspond to transitions from O 1s to the O 2p character [18]. The large band around 1 eV is mainly composed of the O 2p state hybridized with the unoccupied Ta 5d state, though the contribution of Bi 6p state may exist in the conduction band region.

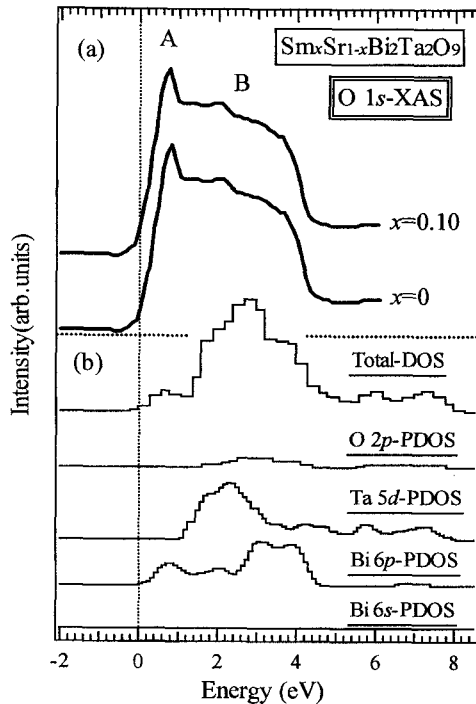


Fig. 3 (a) O 1s XAS spectra of $\text{SrBi}_2\text{Ta}_2\text{O}_9$ and $\text{Sm}_{0.1}\text{Sr}_{0.9}\text{Bi}_2\text{Ta}_2\text{O}_9$ ceramics. (b) Band structure of $\text{SrBi}_2\text{Ta}_2\text{O}_9$ calculated by tight-binding method.

Two features denoted by the A and B peaks are observed in the conduction band. Comparing with the band calculation shown under the XAS spectra, we can estimate that the features A and B of conduction band consist of Bi 6p and Ta 5d states, respectively. Furthermore, the peak positions and bandwidth of total DOS are in good agreement with those of two XAS spectra. However, the intensities of Bi 6p and Ta 5d states do not change by Sm substitution.

Figure 4 shows the O 1s SXES of $\text{SrBi}_2\text{Ta}_2\text{O}_9$ and $\text{Sm}_{0.1}\text{Sr}_{0.9}\text{Bi}_2\text{Ta}_2\text{O}_9$ ceramics. The SXES spectra are normalized by the beam current and measurement time. The clear selection rule of SXES is caused mainly within the same atomic species, because the core hole is strongly localized. For this reason, the O 1s SXES spectrum reflects the O 2p PDOS corresponds to the band structure in the valence band region, since the valence band of $\text{SrBi}_2\text{Ta}_2\text{O}_9$ is mainly composed of O 2p. There is no structure in the energy gap region of $\text{SrBi}_2\text{Ta}_2\text{O}_9$. The three features denoted by the α , β , and χ peaks are observed in the valence band. To further investigate these features observed in the SXES spectra, we have compared with the band calculation. The peak positions and bandwidth of total DOS are in good agreement with those of two SXES spectra. The valence band is mainly composed of O 2p state. The Ta 5d contribution is more significant in the higher energy (feature χ), where the O 2p states have a larger admixture of Ta 5d states. The Bi 6s contribution hybridized with O 2p state is also observed in the top of the valence band. Therefore, the feature β corresponds to the nonbonding state and the feature β corresponds to the bonding state that is well mixed with Ta 5d state.

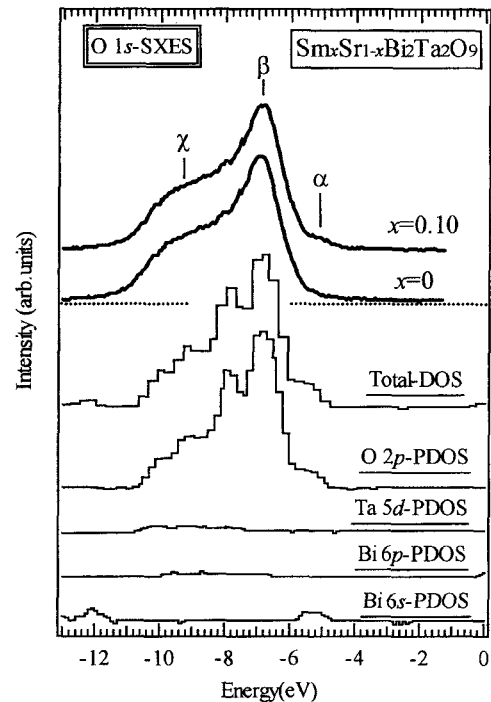


Fig. 4 (a) O 1s SXES spectra of $\text{SrBi}_2\text{Ta}_2\text{O}_9$ and $\text{Sm}_{0.1}\text{Sr}_{0.9}\text{Bi}_2\text{Ta}_2\text{O}_9$ ceramics. (b) Band structure of $\text{SrBi}_2\text{Ta}_2\text{O}_9$ calculated by tight-binding method.

The feature α corresponds to the Bi 6s state hybridized with O 2p state. Comparing either SXES spectra, the intensity of the feature α is higher in $\text{Sm}_{0.1}\text{Sr}_{0.9}\text{Bi}_2\text{Ta}_2\text{O}_9$, indicating that the hybridization effect between Bi and O increases.

The above result indicates that the Bi 6s orbital is fully occupied and acts as a lone pair state. This behavior is similar to the Pb 6s orbital in PbTiO_3 [19, 20]. In $\text{SrBi}_2\text{Ta}_2\text{O}_9$, the Bi state is asymmetric and the Bi lone pair lies off center and points out of the Bi_2O_2 layer, in a fashion similar to the Pb 6s lone pair in PbO . The ferroelectric behavior is amplified by the off-center displacements of the Bi and $\text{SrBi}_2\text{Ta}_2\text{O}_9$ and Pb in PbTiO_3 . The displacements of these ions are considered to be driven by the lone pair s electrons, though the detailed origin has not been clarified in this study.

4. CONCLUSION

We have prepared the dense bulk ceramics of $\text{Sm}_x\text{Sr}_{1-x}\text{Bi}_2\text{Ta}_2\text{O}_9$ and studied its electronic structure by XAS and SXES techniques. The E_c decreases with Sm substitution. The P_r and E_c at $x=0.10$ were $2P_r=20.7 \mu\text{C}/\text{cm}^2$ and $2E_c=30.0 \text{ kV}/\text{cm}$, respectively. The valence band consists of O 2p state hybridized with Ta 5d and Bi 6s states. The conduction band consists of Ta 5d and Bi 6p states. The intensity of the Bi 6s state located at the top of the valence band increases with Sm substitution. This finding is direct evidence that the ferroelectric behavior of $\text{SrBi}_2\text{Ta}_2\text{O}_9$ is driven by Bi with the lone pair s electrons.

ACKNOWLEDGEMENTS

This work was partly supported by the Foundation for Promotion of Material Science and Technology of Japan (MST Foundation), Sumitomo Foundation, and a Grant-In-Aid for Science Research from the Ministry of Education, Culture, Sports, Science and Technology of Japan.

REFERENCES

- [1] C. A. Paz de Araujo, J. D. Cuchiaro, L. D. McMillan, M. C. Scott and J. F. Scott: *Nature (London)* **374** (1995) 627.
- [2] A. D. Rae, J. G. Thompson and R. L. Withers: *Acta Crystallogr., Sect. B: Struct. Sci.* **48** (1992) 418.
- [3] M. Noda, Y. Matsumuro, H. Sugiyama and M. Okuyama: *Jpn. J. Appl. Phys.* **38** (1999) 2275.
- [4] A. Furuya and J. D. Cuchiaro: *Jpn. J. Appl. Phys.* **39** (2000) L371.
- [5] M. J. Forbess, S. Seraji, Y. Wu, C. P. Nguyen and G. Z. Cao: *Appl. Phys. Lett.* **74** (2000) 1904.
- [6] K. Aizawa, E. Tokumitsu, K. Okamoto and H. Ishiwara: *Appl. Phys. Lett.* **76** (2000) 2609.
- [7] T. Noguchi, T. Hase and Y. Miyasaka: *Jpn. J. Appl. Phys.* **35** (1996) 4900.
- [8] K. Miura and M. Tanaka: *Jpn. J. Appl. Phys.* **37** (1998) 2554.
- [9] Y. Shimakawa, Y. Kudo, Y. Nakagawa, T. Kamiyama, H. Asano and F. Izumi: *Appl. Phys. Lett.* **74** (1999) 1904.
- [10] Y. Noguchi, M. Miyayama and T. Kudo: *J. Appl. Phys.* **88** (2000) 2146.
- [11] Y. Noguchi, M. Miyayama and T. Kudo: *Phys. Rev. B* **63** (2001) 214102.
- [12] Y. Noguchi, M. Miyayama, K. Oikawa, T. Kamiyama, M. Osada and M. Kakihana: *Jpn. J. Appl. Phys.* **41** (2002) 7062.
- [13] T. Higuchi, T. Tsukamoto, M. Watanabe, M. M. Grush, T. A. Callcott, R. C. Perera, D. L. Ederer, Y. Tokura, Y. Harada, Y. Tezuka and S. Shin: *Phys. Rev. B* **60** (1999) 7711.
- [14] T. Higuchi, T. Tsukamoto, K. Kobayashi, S. Yamaguchi, Y. Ishiwata, T. Yokoya, M. Fujisawa and S. Shin: *Phys. Rev. B* **61** (2000) 12860.
- [15] T. Higuchi, M. Tanaka, K. Kudoh, T. Takeuchi, Y. Harada, S. Shin and T. Tsukamoto: *Jpn. J. Appl. Phys.* **40** (2001) 5803.
- [16] T. Higuchi, N. Ohtake, N. Machida, S. Shin and T. Tsukamoto: in preparation.
- [17] J. Robertson, C. W. Chen, W. L. Warren and C. D. Gutleben: *Appl. Phys. Lett.* **69** (1996) 1704.
- [18] A. Arranz, V. Perez-Dieste and C. Palacio: *Phys. Rev. B* **66** (2002) 75420.
- [19] R. E. Cohen: *Nature* **358** (1992) 136.
- [20] R. E. Cohen and H. Krakauer: *Phys. Rev. B* **42** (1990) 6416.

(Received October 11, 2003; Accepted March 10, 2004)